

## Oxygen-vacancy ordering and microstructure in annealed $\text{Ba}_2\text{YCu}_3\text{O}_{7-\delta}$ superconductors

D. J. Werder, C. H. Chen, R. J. Cava, and B. Batlogg

*AT&T Bell Laboratories, Murray Hill, New Jersey 07974*

(Received 3 June 1988)

We present the results of a systematic electron diffraction study of short-range oxygen-vacancy ordering in ceramic  $\text{Ba}_2\text{YCu}_3\text{O}_{7-\delta}$  superconductors with  $0.08 \leq \delta \leq 0.67$ , prepared by a Zr-getter technique. In addition to the two types of orderings with reduced wave vectors  $(\frac{1}{2}, 0, 0)$  and  $(\frac{2}{3}, 0, 0)$ , a new vacancy ordering with reduced wave vector  $(\frac{1}{3}, 0, 0)$  has been found. We have observed in samples with  $\delta=0.5$  a vacancy ordering with a large correlation length ( $\sim 150 \text{ \AA}$ ) in the  $c$ -axis direction. We have also observed a tweedlike microstructure at  $\delta=0.61$ , which is caused by a high density of microtwins.

Recently<sup>1</sup> it was shown how the oxygen stoichiometry affects the physical properties of the high- $T_c$  superconductor  $\text{Ba}_2\text{YCu}_3\text{O}_{7-\delta}$ . In particular, a plateau in  $T_c$  at 60 K and minimum in the room-temperature resistivity versus oxygen deficiency  $\delta$ , were found for the range  $0.3 \lesssim \delta \lesssim 0.4$ . These plateaus suggested the existence of oxygen-vacancy ordering. Several groups have shown by electron diffraction<sup>2-5</sup> and by x-ray diffraction<sup>6</sup> the existence of short-range oxygen-vacancy ordering. The diffuse diffraction spots due to ordering were found to lie along the  $a$  axis. Thus, the superlattice wave vector  $Q$  is described by  $Q = (h, k, l) \pm q$ , where  $q$  is the reduced superlattice wave vector, which has the general form  $(n, 0, 0)$ ,  $n$  being some fractional value. In our previous electron diffraction study<sup>2</sup> we found orderings with  $q = (\frac{1}{2}, 0, 0)$  and  $(\frac{2}{3}, 0, 0)$ , with a larger correlation length in the [010] direction than in the [100] direction. The structure was found to be completely uncorrelated along the  $c$  axis. In a more recent<sup>7</sup> study we have found that the ordering is spatially inhomogeneous on a microscopic scale. By real-space dark-field imaging, using the diffuse diffraction spots, we have observed small vacancy-ordered domains in single crystals of  $\text{Ba}_2\text{YCu}_3\text{O}_{6.7}$ , prepared by quenching in  $\text{O}_2$ . These ordered domains were found to have approximate dimensions of  $20 \times 200 \times 10 \text{ \AA}^3$  with the long dimension pointing along the Cu-O chain ([010] direction).

In this paper we present the results of a systematic electron diffraction study of the various short-range oxygen-vacancy orderings found in annealed, ceramic  $\text{Ba}_2\text{YCu}_3\text{O}_{7-\delta}$ . A large correlation length along the  $c$ -axis direction was found in samples with  $\delta=0.5$ . We find a new vacancy ordering with  $q = (\frac{1}{3}, 0, 0)$ . We have also observed a tweedlike microstructure at  $\delta=0.61$ .

Oxygen-deficient samples of bulk  $\text{Ba}_2\text{YCu}_3\text{O}_{7-\delta}$  were prepared by a Zr-getter low-temperature annealing technique. The details of this gettering technique were described elsewhere.<sup>1</sup> The following oxygen deficiencies were studied: 0.08, 0.19, 0.20, 0.28, 0.32, 0.41, 0.51, 0.61, and 0.67. All samples were annealed at  $440^\circ\text{C}$  except  $\delta=0.20$  and  $0.28$ , which were annealed at  $472^\circ\text{C}$ . These samples have also been fully characterized magnetically and by lattice parameter measurements.<sup>8</sup> Samples from

$\delta=0.28$  to  $0.51$  lie within the 60-K plateau of the  $T_c$  vs  $\delta$  curve.  $T_c$  drops from the plateau around  $\delta=0.51$ . The  $T_c=60 \text{ K}$  material exhibited a Meissner effect similar to that observed in the 90-K phase. Samples for transmission electron microscopy and diffraction were prepared by either crushing the bulk samples or by polishing and ion milling with  $\text{Ar}^+$  at 6 kV, and then finishing at 4 kV. No differences were found in the samples prepared by these two methods, as far as diffraction studies were concerned. The samples were studied in a JEOL transmission electron microscope operated at 200 kV.

The oxygen compositions and their corresponding observed vacancy orderings are listed in Table I. All samples showed orthorhombic symmetry as evidenced by the presence of twins. This is consistent with the x-ray measurements.<sup>8</sup> The samples with  $\delta=0.19, 0.20$ , and  $0.61$  showed very weak diffuse streaking with no discernible maxima. This corresponds to a very small volume fraction<sup>7</sup> (on the order of 1% or less) of poorly ordered material. For  $\delta=0.08$  and  $0.67$  grains having diffuse superlattice spots with  $q = (\frac{1}{2}, 0, 0)$  were found but these were not as common as grains with weak diffuse streaks. The majority of the grains in the  $\delta=0.08$  sample had no diffuse streaks. Only samples in the range  $0.28 \leq \delta \leq 0.51$  showed diffuse superlattice spots in every grain observed. The sample with  $\delta=0.32$  showed a new ordering, previously not observed, with a reduced wave

TABLE I. Oxygen-vacancy ordering observed in oxygen-deficient  $\text{Ba}_2\text{YCu}_3\text{O}_{7-\delta}$  ceramics.

$\delta$	Vacancy ordering
0.08	Few grains with $(\frac{1}{2}, 0, 0)$
0.19	Weak diffuse streaking
0.20	Weak diffuse streaking
0.28	$(\frac{2}{3}, 0, 0)$ and $(\frac{1}{2}, 0, 0)$
0.32	$(\frac{1}{3}, 0, 0)$ and $(\frac{1}{2}, 0, 0)$
0.41	$(\frac{1}{2}, 0, 0)$
0.51	$(\frac{1}{2}, 0, 0)$
0.61	Weak diffuse streaking
0.67	Weak diffuse streaking and $(\frac{1}{2}, 0, 0)$

vector  $q = (\frac{1}{3}, 0, 0)$ . As mentioned in our earlier work<sup>2</sup> the sample with  $\delta = 0.28$  showed equally common orderings of  $(\frac{2}{3}, 0, 0)$  and  $(\frac{1}{2}, 0, 0)$ . Some grains in the  $\delta = 0.32$  sample also showed  $(\frac{1}{2}, 0, 0)$  ordering but these were not as common as the  $(\frac{1}{3}, 0, 0)$  ordering. Figure 1 is a [001] zone axis electron diffraction pattern, from one twin domain, showing the  $(\frac{1}{3}, 0, 0)$  ordered spots. A densitometer trace along the [100] direction of Fig. 1 showing intensity maxima at  $(\frac{1}{3}, 0, 0)$  and  $(\frac{2}{3}, 0, 0)$  is presented in Fig. 2, curve *c*. Curves *a* and *b* are the  $(\frac{1}{2}, 0, 0)$  and  $(\frac{2}{5}, 0, 0)$  traces, respectively, from  $\delta = 0.28$ . As can be seen from Table I the preferred oxygen-vacancy ordering in  $\text{Ba}_2\text{YCu}_3\text{O}_{7-\delta}$  is  $(\frac{1}{2}, 0, 0)$ . It should be noted that these superlattice spots due to vacancy ordering are broad with a diffuse tail along the *a* axis and are much sharper along the *b* axis. Although another type of ordering with  $q = (\frac{1}{4}, \frac{1}{4}, 0)$  has been reported from samples quenched from high temperature,<sup>9</sup> we have only observed these three types of ordering, namely,  $(\frac{1}{3}, 0, 0)$ ,  $(\frac{2}{5}, 0, 0)$ , and  $(\frac{1}{2}, 0, 0)$ , in samples that were prepared by the Zr-getter, low-temperature annealing technique. However, we do not expect that this technique gives equilibrium phases but rather a subset of the possible oxygen configurations. These three types of ordering we have observed are consistent with a recent theoretical model proposed by Khachaturyan and Morris,<sup>10</sup> in which they show the ordering wave vector to have the form  $(n/2n+1, 0, 0)$ , where *n* is an integer.

Wille, Berera, and de Fontaine<sup>11</sup> calculated the temperature versus  $\delta$  phase diagram for  $\text{Ba}_2\text{YCu}_3\text{O}_{7-\delta}$ , using the cluster variation method, by choosing the appropriate signs of the anisotropic interactions parameters so as to stabilize the  $(\frac{1}{2}, 0, 0)$  ordered phase. This calculated phase diagram shows that the  $(\frac{1}{2}, 0, 0)$  ordered phase is stable below 450°C. It is expected that the kinetics near this temperature should be fast enough to facilitate the growth of the  $(\frac{1}{2}, 0, 0)$  ordered phase into a macroscopic domain with a good volume fraction. However, in our dark field imaging experiments<sup>7</sup> on single crystals with  $\delta = 0.30$ , we observe only very small ordered domains

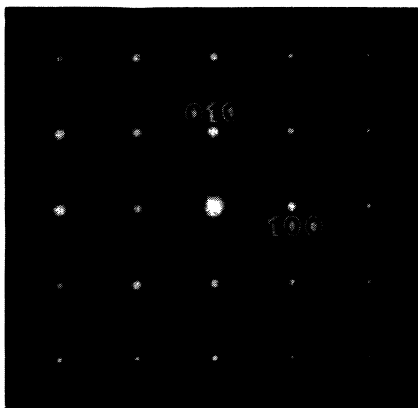


FIG. 1. An [001] zone axis electron diffraction pattern, from one twin domain, showing  $(\frac{1}{3}, 0, 0)$  ordering. For this sample  $\delta = 0.32$ .

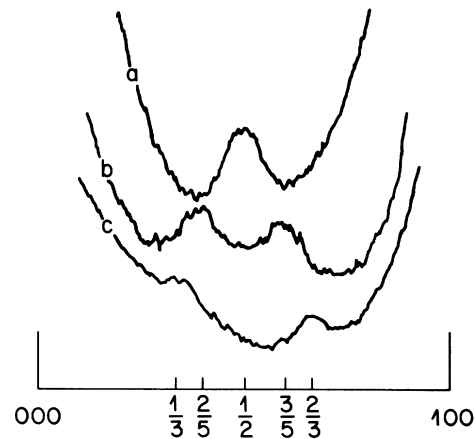


FIG. 2. Curve *c* is a densitometer trace along the [100] direction of Fig. 1, showing intensity maxima at  $(\frac{1}{3}, 0, 0)$  and  $(\frac{2}{3}, 0, 0)$ . Curves *a* and *b* are traces from two different grains in the same sample ( $\delta = 0.28$ ) showing  $(\frac{1}{2}, 0, 0)$  and  $(\frac{2}{5}, 0, 0)$  ordering, respectively.

comprising at most 10% of the sample volume. Our present diffraction studies on the ceramics also suggest small vacancy-ordered domains and small volume fractions.<sup>12</sup> Khachaturyan and Morris,<sup>10</sup> on the other hand, calculate the phase diagram by a different configurational thermodynamic method. They obtain in the phase diagram a two-phase tetragonal-orthorhombic region capped by a miscibility gap at  $\sim 130^\circ\text{C}$ . We have not observed any large-scale ( $> 100 \text{ \AA}$ ) phase separation of tetragonal and orthorhombic symmetries. Our samples, on a macroscopic scale, contain only orthorhombic phases. The miscibility gap contains two orthorhombic phases, though the calculation does not take into account any ordered structure. The authors propose<sup>10</sup> that the orthorhombic ordered phases with  $q = (n/2n+1, 0, 0)$ , *n* being an integer, are transient metastable and that because of the slow kinetics these phases should be difficult to grow to macroscopic size.

In previous diffraction studies,<sup>2-6</sup> it was shown that the correlation length of the vacancy-ordered structure along the *c* axis is short. The correlation length is found to be on the order of the *c*-axis lattice parameter ( $\sim 11 \text{ \AA}$ ). In electron diffraction patterns this appears as a ribbon of diffuse intensity along the  $c^*$  direction in [010] zone axis patterns. It was also shown<sup>6,7</sup> that the correlation length along the *a* axis is  $\sim 20 \text{ \AA}$ . We have found, for  $\delta = 0.51$ , large correlation lengths along both the *a* and *c* axes. The correlation lengths in both the *a* and *c* axes were found to be  $\sim 150 \text{ \AA}$ . The *b*-axis correlation length is of similar dimension ( $\geq 200 \text{ \AA}$ ) as that found previously.<sup>7</sup> Figure 3(a) is a [001] zone axis pattern showing the sharp  $(\frac{1}{2}, 0, 0)$  superlattice spots for  $\delta = 0.51$ . The superlattice spots appear in both directions because the selected area diffraction aperture covered more than one twin domain. Since the *a* and *b* axes are mirrored across a twin boundary<sup>13</sup> superlattice spots appear in both directions. In Fig. 3(b) we show the [010] zone axis pattern of the new ordered structure with a large *c*-axis correlation length.

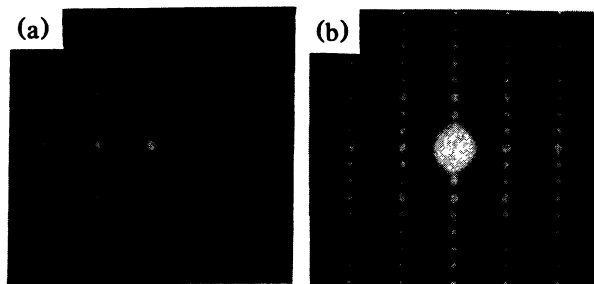


FIG. 3. (a) is an [001] zone axis pattern showing  $(\frac{1}{2}, 0, 0)$  ordering for  $\delta=0.51$ . (b) is an [010] zone axis pattern for the same sample. Note the sharp superlattice spots at the  $(\frac{1}{2}, 0, l)$  positions.

This pattern was obtained from the same sample as Fig. 3(a). Note the sharp superlattice spots at the  $(\frac{1}{2}, 0, l)$  positions. A sample annealed at  $415^\circ\text{C}$  with  $\delta=0.50$  also showed this large  $c$ -axis correlation length, but the superlattice spots were much weaker than the sample annealed at  $440^\circ\text{C}$ . The cause of this strong interaction between vacancies at such a large distance ( $c$  axis) is not known at this time. It may be that the Ba plays a central role in this interaction. Configuration interaction calculations for neighbors along the  $c$  axis, such as those by Wille, Berera, and de Fontaine<sup>11</sup> for vacancies in the basal plane, may shed light on this large correlation.

In this series of samples we have also observed a tweed-like microstructure at  $\delta=0.61$ , which is caused by a high density of microtwins ( $\lesssim 200 \text{ \AA}$ ). This tweed contrast, shown in Fig. 3, is caused by the presence of microtwins in both the [110] and  $[1\bar{1}0]$  directions. The micrograph in Fig. 4(a) was taken, under two-beam condition, with the reciprocal-lattice vector  $g=(2,0,0)$ . Here, contrast from microtwins in both directions is visible. In Fig. 4(b), taken with  $g=(2,2,0)$ , there is no contrast from those microtwins perpendicular to the  $g$  vector. This contrast is as would be expected for twin structures since we can define a Burgers vector in the twin plane. Also seen in Fig. 4 are the normal macrotwins ( $\sim 2000 \text{ \AA}$ ) found in orthorhombic  $\text{Ba}_2\text{YCu}_3\text{O}_{7-\delta}$ .

This tweed contrast was only found in the sample with  $\delta=0.61$ . This  $\delta$  must represent a region of oxygen

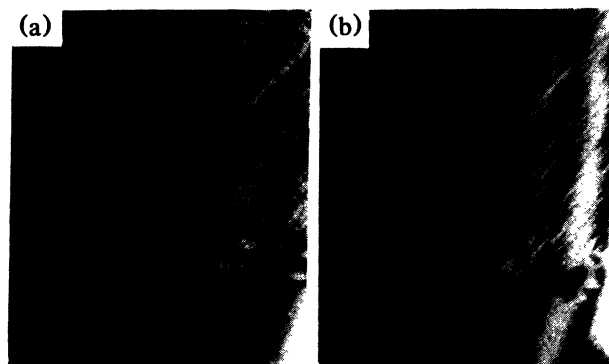


FIG. 4. Dark field electron micrographs from the [001] zone axis direction, showing microtwins in sample with  $\delta=0.61$ . The reciprocal-lattice vector  $g$  used in (a) is  $(2,0,0)$  and in (b)  $(2,2,0)$ . The arrows point to dislocations.

deficiency where lattice strain is close to a maximum. To relieve this strain a large density of microtwins have formed. A large number of dislocations (marked with arrows in Fig. 4) were also found in this sample, presumably to further help relieve strain. We also mention that this tweed, microtwin structure has been formed in *in situ* heating experiments, by us<sup>14</sup> and in Ref. 15, though a correlation with oxygen composition could not be made.

In conclusion, we have presented the results of a systematic electron diffraction study of annealed, ceramic  $\text{Ba}_2\text{YCu}_3\text{O}_{7-\delta}$ , for  $0.08 \leq \delta \leq 0.67$ . We have shown for the first time a large correlation length for oxygen vacancies along the  $c$  axis. The reason for this long-distance vacancy interaction is not known. For  $\delta=0.32$  we have found a new vacancy ordering at  $(\frac{1}{3}, 0, 0)$ , it is also shown that  $(\frac{1}{2}, 0, 0)$  ordering is preferred in this system. Finally, we have also observed a tweedlike microstructure at  $\delta=0.61$ , which is caused by a high density of microtwins.

We would like to thank K. Rabe and S. Nakahara for helpful discussions. We would also like to thank D. de Fontaine and A. G. Khachaturyan for copies of their unpublished work and also for reprints of their published work.

<sup>1</sup>R. J. Cava, B. Batlogg, C. H. Chen, E. A. Rietman, S. M. Zahurak, and D. J. Werder, *Nature* **329**, 423 (1987); *Phys. Rev. B* **36**, 5719 (1987).

<sup>2</sup>D. J. Werder, C. H. Chen, R. J. Cava, and B. Batlogg, *Phys. Rev. B* **37**, 2317 (1988).

<sup>3</sup>C. Chaillout, M. A. Alario-Franco, J. J. Capponi, J. Chenavas, J. L. Hodeau, and M. Marezio, *Phys. Rev. B* **36**, 7118 (1987).

<sup>4</sup>H. W. Zandbergen, G. Van Tendeloo, T. Okabe, and S. Amelinckx, *Phys. Status Solidi (a)* **103**, 45 (1987).

<sup>5</sup>M. Tanaka, M. Terauchi, K. Tsuda, and A. Ono, *Jap. J. Appl. Phys.* **26**, L1237 (1987).

<sup>6</sup>R. M. Fleming, L. F. Schneemeyer, P. K. Gallagher,

B. Batlogg, L. W. Rupp, and J. V. Waszczak, *Phys. Rev. B* **37**, 7920 (1988).

<sup>7</sup>C. H. Chen, D. J. Werder, L. F. Schneemeyer, P. K. Gallagher, and J. V. Waszczak, *Phys. Rev. B* **38**, 2888 (1988).

<sup>8</sup>R. J. Cava, B. Batlogg, S. A. Sunshine, T. Siegrist, R. M. Fleming, K. Rabe, L. F. Schneemeyer, D. W. Murphy, R. B. van Dover, P. K. Gallagher, S. H. Glarum, S. Nakahara, R. C. Farrow, J. J. Krajewski, S. M. Zahurak, J. V. Waszczak, J. H. Marshall, P. Marsh, L. W. Rupp, Jr., W. F. Peck, and E. A. Reitman, in *Proceedings of the International Conference on High-Temperature Superconductors and Materials and Mechanisms of Superconductivity, Interlaken*,

- Switzerland 1988*, edited by J. Müller and J. L. Olsen [Physica C **153–155**, 560 (1988)].
- <sup>9</sup>M. A. Alario-Franco, J. J. Capponi, C. Chaillout, J. Chenavas, and M. Marezio, *Mater. Res. Soc. Symp. Proc.* **99**, 41 (1988).
- <sup>10</sup>A. G. Khaxhaturyan and J. W. Morris, Jr., *Phys. Rev. Lett.* **61**, 215 (1988).
- <sup>11</sup>L. T. Wille, A. Berera, and D. de Fontaine, *Phys. Rev. Lett.* **60**, 1065 (1988).
- <sup>12</sup>The intensity of the superlattice spots in the ceramics was much weaker than in the single crystals, therefore, making dark field imaging difficult. Since the cause of the superlattice spots in the single crystals should be due to the same mechanism as in the ceramics, intensity differences between these two materials should be caused by differing volume fractions of ordered material and not by structure factor differences. Thus, we have extrapolated from the single crystals to the ceramics.
- <sup>13</sup>C. H. Chen, D. J. Werder, J. R. Kwo, S. H. Liou, and M. Hong, *Phys. Rev. B* **35**, 8767 (1987).
- <sup>14</sup>Heating experiments were done in the microscope using a heating stage with a thermocouple, as opposed to electron-beam heating. Microtwins formed at  $\sim 500^\circ\text{C}$ .
- <sup>15</sup>S. Nakahara (unpublished).

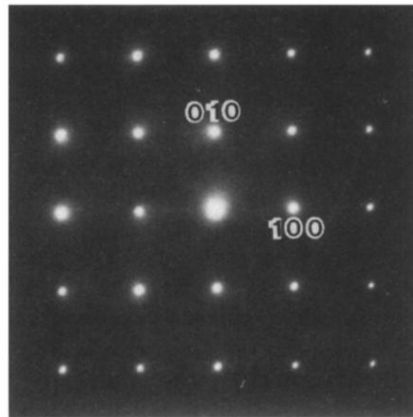


FIG. 1. An [001] zone axis electron diffraction pattern, from one twin domain, showing  $(\frac{1}{3}, 0, 0)$  ordering. For this sample  $\delta=0.32$ .

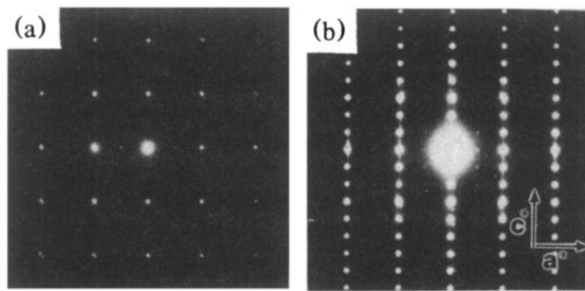


FIG. 3. (a) is an [001] zone axis pattern showing  $(\frac{1}{2}, 0, 0)$  ordering for  $\delta = 0.51$ . (b) is an [010] zone axis pattern for the same sample. Note the sharp superlattice spots at the  $(\frac{1}{2}, 0, l)$  positions.

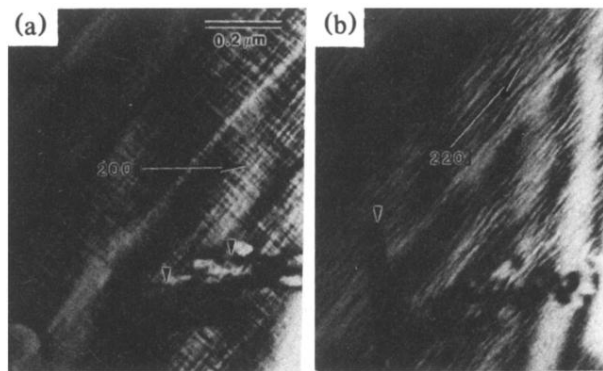


FIG. 4. Dark field electron micrographs from the [001] zone axis direction, showing microtwins in sample with  $\delta=0.61$ . The reciprocal-lattice vector  $g$  used in (a) is (2,0,0) and in (b) (2,2,0). The arrows point to dislocations.